Kufa Journal of Pharmaceutical Sciences

© 2025- KJPS | Volume 02 | Issue 02 | Print ISSN: 3005-7833

Design, Synthesis, and Biological Evaluation of Isatin-Based 3-Phenoxybenzoic Acid Derivatives as VEGFR-2 Inhibitors with Anti-Angiogenic Potential

Faidh Yahya Ahmed[1*], Ammar Abdul Aziz[1]

[1]*Department of Pharmaceutical Chemistry, Faculty of Pharmacy, University of Kufa, Najaf, Iraq*

[2]*Department of Pharmaceutical Chemistry, Faculty of Pharmacy, University of Kufa, Najaf, Iraq*

ABSTRACT

Objectives: Due to its significant role in supporting the development and spread of cancer, the inhibition of vascular endothelial growth factor receptor 2 (VEGFR-2) of angiogenesis has been used in cancer treatment. The research presented created and synthesized a number of phenoxy benzoic acid derivatives. This work develops and evaluates four novel drugs targeting cancer and the VEGFR. For the chemical synthesis, we used phenoxy benzoic acid, sulphuric acid, methanol, hydrazine hydrate, Isatin derivatives, and glacial acetic acid. In vitro cell line investigations and in silico docking studies showed antitumor efficacy for the produced substances. The results demonstrated that the inclusion of isatin in the molecular framework enhanced receptor binding by interacting with critical amino acids essential for VEGFR-2 enzymatic activity. The docking study showed that compounds F1 and F4 had the highest binding affinities, with S-scores of -8.54 and -8.2, respectively, interacting with key amino acids such as Glu885, Cys1045, and Asp1046. The in vitro cytotoxicity results demonstrated selective anticancer activity. Compound F4 exhibited the highest potency against MCF-7 cells (IC50 = 5.76 µM), while F1 displayed notable activity against HepG2 cells (IC50 = 9.73 µM). Compared to sorafenib, the synthesized compounds showed selective cytotoxicity toward cancer cells while sparing normal cells. These findings suggest that the newly synthesized compounds could be potential VEGFR-2 inhibitors with selective anticancer properties. In conclusion, the synthesized Isatin-based 3-phenoxybenzoic acid derivatives exhibited strong VEGFR-2 inhibitory activity and selective cytotoxicity against cancer cells while reducing toxicity to normal cells.

Keywords: Angiogenesis; Cancer; VEGFR-2; Isatin; MCF-7; HepG-2

I. INTRODUCTION

Cancer is a degenerative disease characterized by unregulated and excessive cell differentiation and proliferation, with the potential for these cells to metastasize to other regions of the body, resulting in mortality [1-4]. In 2020 alone, there were around 10.3 million cancer-related deaths and 19.3 million new cases, making cancer one of the top causes of death globally [5]. Consequently, developing superior anticancer medicines is imperative, particularly those exhibiting powerful biological activity, enzyme inhibitory effects, and little toxicity [6,7]. The rising prevalence of cancer cases is mostly attributed to the resistance of cancer cells to existing treatments, prompting research to identify new targets or develop novel chemical scaffolds to interact with previously recognized targets [8]. Vascular Endothelial Growth Factor (VEGF) has been identified as a major modulator of tumor angiogenesis. VEGF triggers the activation and proliferation of endothelial cells [9].

However, the development and advancement of pathological diseases are linked to either insufficient or excessive angiogenesis [13]. Excessive angiogenesis has been identified as a key therapeutic target for inflammatory, neoplastic, and autoimmune diseases. A major therapeutic problem, pathological angiogenesis has severe, undesired negative consequences on normal organ function [14]. The VEGF signaling system fundamentally regulates tumor angiogenesis. VEGF has been confirmed as a therapeutic target in a number of human cancer types

KJPS | E- mail: phar.kjps@uokufa.edu.iq | Received: 05/05/2025 | Accepted: 06/07/2025

*Corresponding author E-mail: faidhy.kamalaldeen@student.uokufa.edu.iq

[15]. VEGFR-2 is regarded as the most significant transducer of VEGF-dependent angiogenesis as it is a prominent target of angiogenesis-related kinases [16]. Therefore, blocking the VEGF/VEGFR signaling pathway is thought to be a promising therapeutic target for preventing tumor angiogenesis and the growth that follows [17]. VEGFR-2 is present on the surface of tumor cells and is highly expressed in tumor-associated endothelial cells, where it regulates angiogenesis that promotes tumor development [18,19]. A powerful VEGFR-2 inhibitor, sorafenib (Nexavar)® is authorized as an antiangiogenic medication [20]. When the structure-activity relationship of the FDA-approved VEGFR-2 inhibitors was examined, four features were found to be almost identical: (a) a heterocyclic head with at least one nitrogen atom to occupy the hinge region of the active site; (b) a spacer to occupy the gatekeeper region; (c) a pharmacophore or hydrogen bonding moiety that forms the necessary H-bonds with the DFG amino acids; and (d) a hydrophobic tail that fills the receptor's allosteric site [21-25]. Benzoic acid derivatives belonging to the diaryl/diphenyl ether class have antimicrobial, antifouling, and antiproliferative properties [26]. Diphenyl derivative bioisosteric analogues interact with many biotarget families. These derivatives' unique qualities stem from their electron and spatial characteristics; the substituents added to the fundamental structure enable these derivatives to adhere to various targets more easily. Consequently, a wide range of pharmacological actions and the polyfunctional effects of derivatives are strengthened [27]. Among the most promising heterocyclic pharmacophore moieties, the favored indolin-2-one scaffold binds to the hinge region in the ATP active pocket of VEGFR-2. Consequently, our target molecules' heterocyclic aromatic ring system was chosen as the indolin-2-one nucleus [28].

II. Experimental section

Materials and Procedures

Sigma-Aldrich, Germany; Riedel de Haën, Germany; Hangzhou Hyper Chemicals; and Merck, Germany, supplied all reagents and anhydrous solvents. The melting points were obtained using the capillary tube technique and the Thomas Hover instrument. The produced compounds were purified, their retention factor (Rf) values were evaluated, and the reaction steps were validated using ascending thin-layer chromatography. This was achieved using a mobile phase of methanol and chloroform in a nine-to-one ratio [29]. KBr discs and a Japanese Shimadzu spectrophotometer were used to scan FT-IR and estimate spectra. Using DMSO as the solvent, H1NMR recordings were conducted at the University of Mashhad using a Bruker 400 MHz apparatus.

Standard protocol for the reactions

First, we dissolved 3-Phenoxybenzoic acid in a methanol solvent and added a few drops of sulfuric acid to the solution to form methyl 3-Phenoxybenzoate. 3-Phenoxybenzoate reacted with hydrazine hydrate, which resulted in the creation of hydrazide. In the presence of glacial acetic acid acting as a catalyst, the hydrazide reacted with aromatic ketone derivatives to produce imines. Scheme 1 outlines the steps in producing compounds (F1–F4) made from 3-phenoxybenzoic acid.

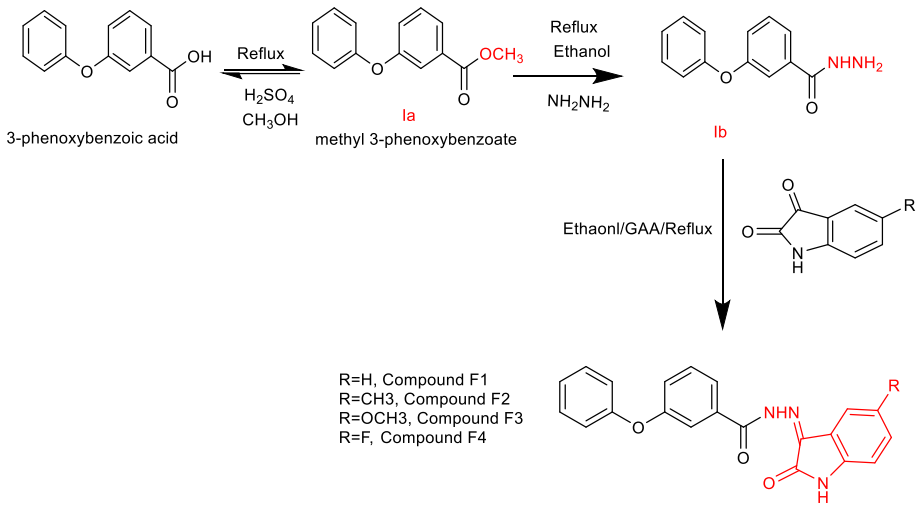

Scheme 1: Synthesis of target compounds (F1-F4).

Synthesis of Methyl 3-Phenoxybenzoate (compound Ia) [30];

In a round-bottom flask, 3-Phenoxybenzoic acid (2 g, 9.34 mmol) was dissolved in 20 mL of methanol. A few drops of sulfuric acid were added to the reaction mixture, which was refluxed for 4 hours. After completion, the solvent was evaporated, and the resulting oil was collected and repeatedly washed with diethyl ether. Subsequently, 20 mL of ethyl acetate was added to the reaction mixture. The organic layer was washed thrice with 20 mL of a 10% sodium bicarbonate solution and once with 10 mL of water. It was then dried over anhydrous magnesium sulfate and filtered to obtain a clear ethyl acetate solution of the product. The solvent was evaporated, yielding an oily compound (Ia). The yield percentage, physical characteristics, and R_f values are shown in **Table 1.**

Synthesis of 3-Phenoxybenzohydrazide (compound Ib) [31];

Compound (Ia) (1.5g, 6.57 mmol) was dissolved in absolute ethanol and then transferred to a round-bottom flask. A solution of hydrazine hydrate 99% (0.96ml, 19.71mmol) was added to the flask, and the resulting reaction mixture was refluxed for 10 hours at 75°C. Upon completion of the reaction, the solvent was evaporated to half of its original volume. After cooling, a white solid product was obtained, filtered, dried, and further purified through ethanol recrystallization, forming a compound (Ib). The yield percentage, physical characteristics, and R_f values are shown in **Table 1.**

2-oxoindolin-3-ylidene-3-phenoxybenzohydrazide (compounds F1-4) [32];

Five drops of glacial acetic acid were carefully incorporated into a reaction mixture consisting of compound (Ib) (0.5 g, 2.19mmol) and an equivalent amount (2.19mmol) of the specified Isatin derivatives from **table 2**, all dissolved in methanol (25 mL). The reaction mixture was then subjected to reflux for 2-3 hours. Subsequently, the resulting precipitate was filtered and recrystallized from ethanol, yielding compounds (F1-4). The yield percentage, physical characteristics, and R_f values are shown in **Table 1.**

Table 2: Types and quantities of isatin derivatives employed in the above reaction.

Isatin derivatives	Number of grams
5-Methylisatin	0.35
Isatin	0.32
5-Methoxyisatin	0.39
5-Floroisatin	0.36

Table 1: The target compounds and their intermediates' physicochemical properties and description.

Compounds and intermediates	Empirical formula	Molecular weight (g/mol)	Description	% Yield	Melting point ^{0}C	R_f value
Ia	$C_{14}H_{12}O_3$	228.25	Yellow oil	89	-----	0.75
Ib	$C_{13}H_{12}N_2O_2$	228.25	White crystals	92	104-106	0.6
F1	$C_{21}H_{15}N_3O_3$	357.37	Yellow crystals	86	238-240	0.81
F2	$C_{22}H_{17}N_3O_3$	371.40	Yellow crystals	82	257-259	0.58
F3	$C_{22}H_{17}N_3O_4$	387.40	Brown crystals	53	221-223	0.76
F4	$C_{21}H_{14}FN_3O_3$	375.36	Orange crystals	93	289-291	0.80

Spectroscopic analysis

Compound Ia ($C_{14}H_{12}O_3$) **FT-IR (cm^{-1})** 3061 (C-H stretching of aromatic), 1722 (C=O of ester), 1585 and 1485 (C=C of aromatic ring) and 1286,1224(C-O stretching of ester). **Compound Ib** ($C_{13}H_{12}N_2O_2$) **FT-IR (cm^{-1})** 3296 and 3155 (N-H stretching broad, indicating hydrogen bonding typical of hydrazones), 1620 (C=O of amide). **Compound F1** ($C_{21}H_{15}N_3O_3$ **FT-IR (cm^{-1})** 3464 (N-H stretching of Isatin), 3219 (N-H stretching of secondary amine), 3061 (C-H stretching of aromatic), 1667 (C=O stretching vibration of amide), 1625 (C=N stretching vibration of imine). **Compound F2** ($C_{22}H_{17}N_3O_3$ **FT-IR (cm^{-1})** 3485 (N-H stretching of Isatin), 3267 (N-H stretching of secondary amine), 3055 (C-H stretching of aromatic), 1685 (C=O stretching vibration of amide), 1627 (C=N stretching vibration of imine). **Compound F3** ($C_{22}H_{17}N_3O_4$ **FT-IR (cm^{-1})** 3480 (N-H stretching of Isatin), 3267 (N-H stretching of secondary amine), 3086 (C-H stretching of aromatic), 1680 (C=O stretching vibration of amide), 1620 (C=N stretching vibration of imine). **Compound F4** ($C_{21}H_{14}FN_3O_3$ **FT-IR (cm^{-1})** 3479 (N-H stretching of Isatin), 3215 (N-H stretching of secondary amine), 3057 (C-H stretching of aromatic), 1678 (C=O stretching vibration of amide), 1631 (C=N stretching vibration of imine). **^{1}H NMR (ppm): Compound F1** 6.94-7-65 (13H, M, Aromatic CH);

11.40 (1H, S, NH); 13.94 (1H, S, NH). **Compound F2 ^{1}H NMR (ppm):** 2.31(3H, S, CH_3); 6.84-7-66 (12H, M, Aromatic CH); 11.30 (1H, S, NH); 13.95 (1H, S, NH). **^{1}H NMR (ppm): Compound F3:** 3.75(3H, S, CH_3); 6.60-7-82 (12H, M, Aromatic CH); 11.20 (1H, S, NH); 13.96 (1H, S, NH). **^{1}H NMR (ppm) Compound F4:** 6.91-7-62 (12H, M, Aromatic CH); 11.41 (1H, S, NH); 13.91(1H, S, NH).

Docking Study

The research used the MOE (Molecular Operating Environment) software version 2015.10 to perform molecular docking analysis, which included preparing the structures of proteins and ligands. We accurately drew the ligand structures using ChemDraw Professional 12.0. Next, we added partial charges and protonated the ligands in their three-dimensional structure in MOE [33]. We then carried out energy minimization. The Protein Data Bank database provided the structure of VEGFR-2 (PDB code: 4ASE), which was then put into MOE for examination. Finding and removing tiny molecules and non-functional chain sequences was part of isolating the target protein. The protein's atomic potentials were altered, and hydrogen bonds were added. Following identifying the active site, the docking procedure is completed by importing the previously produced ligands into MOE.

Cytotoxic Study

In the cytotoxic study, we used four types of cells, MCF7, HepG2, HUVEC, and MCF10a, representing malignant and benign breast cells. Two distinct medium types, RPMI-1640 and DMEM, were used for cell culture. Ten percent fetal bovine serum (FBS) and antibiotics, specifically penicillin at 100 U/mL and streptomycin at 100 µg/mL, were added to both mediums. The cells were kept in a controlled atmosphere at 37 °C, with 5% CO_2 and suitable humidity levels. Trypsin/EDTA and a phosphate-buffered saline (PBS) solution were utilized for cell passage. We employed identical culture conditions and medium for cultivating 3D colonies, as we did for regular monolayer cell culture. The MTT assay was used to evaluate cell growth and viability. The cells were separated using trypsin and counted to conduct a monolayer cell culture. They were then seeded into 96-well plates with 200 µl of new media at a density of 1.4 x 10^4 cells/well. After forming a monolayer, the cells were subjected to different concentrations of compounds (ranging from 600µg/mL to 7.4 µg/mL) for 24 hours at a temperature of 37 °C with a CO_2 concentration of 5%. After the treatment, we separated the liquid part and incubated the cells with a solution of MTT (0.5 mg/mL in PBS) for an extra 4 hours at a temperature of 37 °C. As a result, the liquid above the solid was substituted with dimethyl sulfoxide (100 µL per well), and the cells were placed on a shaking device at 37 °C until the solid entirely dissolved. The ELISA reader was utilized to measure the absorbance at 570 nm to ascertain the viability of the cells. Analyzing the relevant dose-response curves allowed us to estimate the IC50, the quantity of compounds that cause 50% cell death.

II. RESULTS AND DISCUSSION

Chemistry

The methyl ester of 3-phenoxybenzoic acid was obtained via esterification. The wide OH group of the carboxylic acid has vanished, and 3-phenoxybenzoic acid has been changed into methyl 3-phenoxybenzoate, as shown by the existence of a 1722 cm^{-1} carbonyl band (for ester). The resultant ester was reacted with hydrated hydrazine to produce hydrazide. The ester's carbonyl group disappeared at 1722 cm^{-1}, and the appearance of the C=O stretching vibration of amide from 1614 cm^{-1}. Also, new peaks in 3296 cm^{-1} and 3155 cm^{-1} for NH stretching vibration. By reacting molecule (Ib) with suitable ketones in the presence of a catalyst, Schiff base formation was used to synthesize compounds (F1-4). FT-IR in the 1600–1640 cm^{-1} range has proven the development of imine bonds and the absence of carbonyl bonds for ketones.

Cytotoxic Evaluation

Using MTT tests on cell lines, we assessed the cytotoxicity of compounds (F1, F2, F3, and F4). In contrast to sorafenib, the cytotoxic activity of the four synthesized compounds (F1–F4) was assessed against the human umbilical vein endothelial (HUVEC), hepatocellular carcinoma (HepG2), breast cancer (MCF7), and normal breast cells (MCF10a) cell lines. to evaluate our synthesized substances' effects. We calculated the IC50 for every drug or the concentration at which cell viability is reduced by 50%.

Table 3. The reference medication and its derivatives of 3-phenoxybenzoic acid exhibited cytotoxic action (IC50, μM) against MCF7, HepG2, MCF10a, and HUVEC.

Compound	MCF7, IC50(μM)	HepG2, IC50(μM)	MCF10a, IC50(μM)	HUVEC, IC_{50}(μM)
Sorafenib	2.22	13.64	3.55	16.81
F1	9.02	9.73	4661.19	500.88
F2	12.43	24.32	4111.77	420.34
F3	16.14	12.79	451.90	345.49
F4	5.76	18.6	3092.00	229.04

According to the data, every synthesized molecule showed an inhibitory effect and could become a powerful anticancer drug. The findings reveal distinct variations in potency and selectivity among the synthesized compounds. Against **MCF7 cells**, sorafenib exhibited the highest cytotoxicity with an IC50 of **2.22 μM**. Among the synthesized compounds, **F4** (fluorine-substituted) demonstrated the highest potency (IC50 = **5.76 μM**), suggesting a promising anticancer potential. **F1**, **F2**, and **F3** exhibited higher IC50 values (**9.02 μM, 12.43 μM, and 16.14 μM**, respectively), indicating lower potency than sorafenib. However, the selectivity index must also be considered to determine therapeutic potential. Selectivity against normal cells **(MCF10a and HUVEC)** is crucial in assessing drug safety. Sorafenib exhibited an IC50 of **3.55 μM** against **MCF10a**, whereas all synthesized compounds had significantly higher IC50 values, particularly **F1 and F2 (>4000 μM)**, suggesting much lower toxicity to normal breast cells. Similarly, against **HUVEC cells**, sorafenib had an IC50 of **16.81 μM**, while **F1, F2, F3, and F4** exhibited much higher IC50 values, with **F4** showing the lowest **(229.04 μM).** These findings indicate that the synthesized compounds may offer a better therapeutic window with reduced cytotoxic effects on normal cells. Regarding **hepatocellular carcinoma (HepG2),** sorafenib displayed an IC50 of **13.64 μM**. Interestingly, **F1 (9.73 μM) and F3 (12.79 μM)** demonstrated comparable or superior cytotoxicity, suggesting their potential as VEGFR2 inhibitors with hepatocellular carcinoma-targeting capabilities. **F2 and F4** exhibited higher IC50 values (**24.32 μM and 18.67 μM,** respectively), indicating lower potency. Overall, **F4** exhibited the best anticancer activity among the synthesized compounds, particularly against **MCF7 cells**, while maintaining a high selectivity index against normal cells. **F1** also demonstrated promising activity against **HepG2 cells**. The variations in cytotoxicity may be attributed to structural modifications influencing interactions with VEGFR2 and other molecular targets. Further studies, including

molecular docking, enzymatic inhibition, and in vivo assessments, are necessary to validate these findings and optimize the pharmacokinetic profiles of the synthesized compounds.

Docking Study

Molecular docking was used to examine the newly synthesized compounds' binding mechanism and interactions with the essential amino acids in the VEGFR-2 active site to explain their potential VEGFR-2 inhibitory activity. There are several crystal structures for VEGFR-2 in the protein data bank; we chose one for this study (PDB ID: 4ASE). The findings showed that different synthetic compounds had different binding affinities; compounds F1 and F4 showed stronger interactions with the target protein than sorafenib. The molecular docking investigation revealed a predicted binding pattern for all synthesized compounds, which included fitting the NH moiety in the center of the active site at the interface between the allosteric hydrophobic back pocket and the ATP binding site. Interaction occurs through hydrogen bonding between Asp1046 and the side chain carboxylate of Glu885. Additionally, the potential VEGFR-2 inhibitory activity of the newly synthesized compounds is achieved via a hydrophobic contact between the hydrophobic portions of the compounds and the hydrophobic rear pocket, which is lined with the hydrophobic side chains. F1 and F4 had the highest S-scores, measuring approximately -8.5 and 8.2, respectively. This high S. score may be due to additional hydrophobic interaction with Val848 and Val899 in F1, and in F2, the fluorine substituent may enhance binding specificity by forming hydrophobic interactions with nearby residues. The compounds F2 and F3 show lower S. scores than both compounds F1 and F4 and sorafenib. However, they are still effective as they bind to important amino acids in both active sites and an allosteric pocket with improved selectivity by reducing flexibility in the linker to ensure it fits better within the kinase's inactive conformation. **Table 4** shows the synthesized compound's S. score, Rmsd, binding amino acids, and the reference sorafenib.

Table 4: S scores and rmsd values for the substances under investigation.

Name	R group	S-score	Rmsd	Total affinity sites	Molecules that are involved in binding
Sorafenib	-------	-8.24	1.8	4	Glu885, Cys1045, Asp1046, Arg1027.
F1	H	-8.54	1.96	5	Val848, Val899, Glu885, Cys1045, Asp1046.
F2	CH_3	-7.82	1.57	4	Glu885, Leu889, Cys1045, Asp1046.
F3	OCH_3	-7.16	1.80	6	Lys868, Glu885, Lue889, His1026, Cys1045, Asp1046.
F4	F	-8.2	1.07	5	Leu840, Glu885, Leu889, Cys1045, Asp1046.

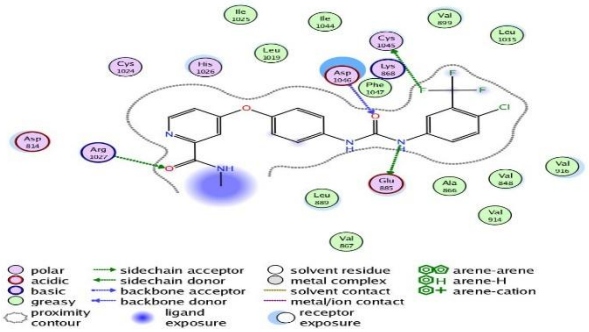

Figure 1: Sorafenib in combination with VEGFR 2 (PDB code: 4ASE) (2D).

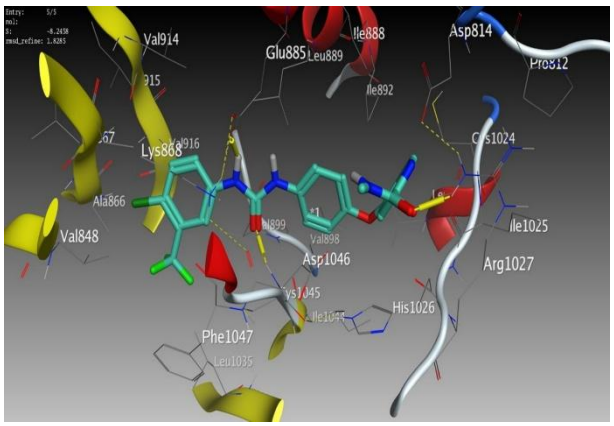

Figure 2: Sorafenib in combination with VEGFR 2 (PDB code: 4ASE) (3D).

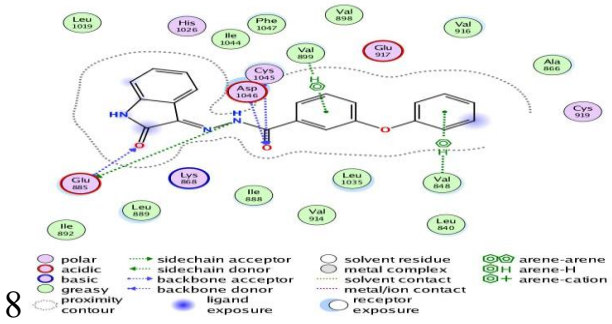

Figure 3: F1 in combination with VEGFR 2 (PDB code: 4ASE) (2D).

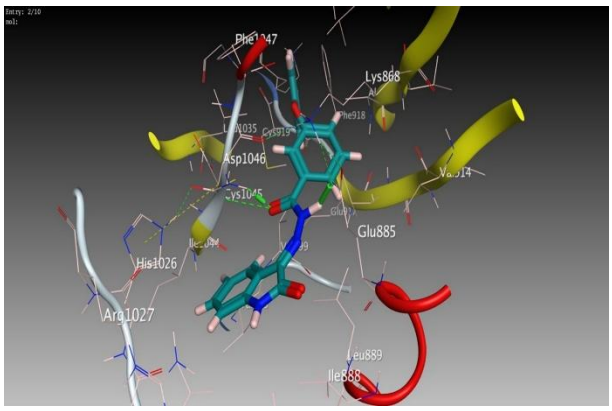

Figure 4: F1 in combination with VEGFR 2 (PDB code: 4ASE) (3D).

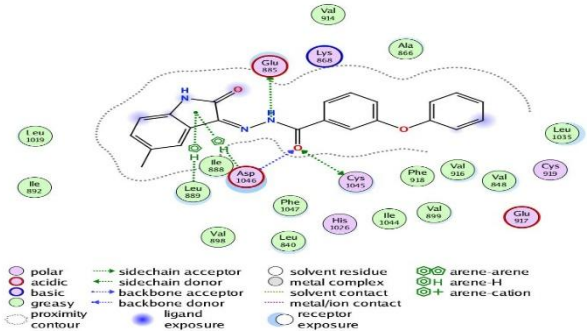

Figure 5: F2 in combination with VEGFR 2 (PDB code: 4ASE) (2D).

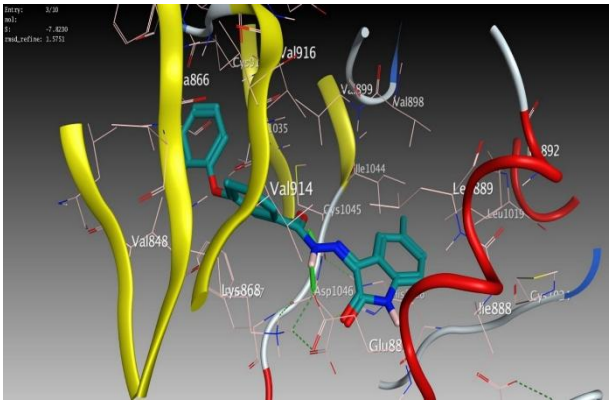

Figure 6: F2 in combination with VEGFR 2 (PDB code: 4ASE) (3D).

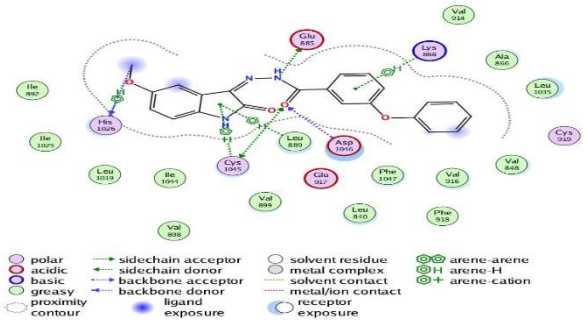

Figure 7: F3 in combination with VEGFR 2 (PDB code: 4ASE) (2D).

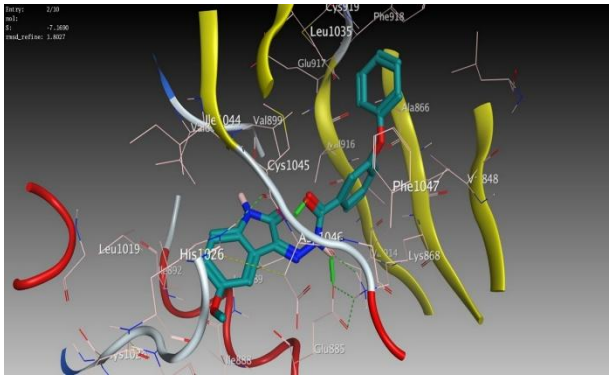

Figure 8: F3 in combination with VEGFR 2 (PDB code: 4ASE) (3D).

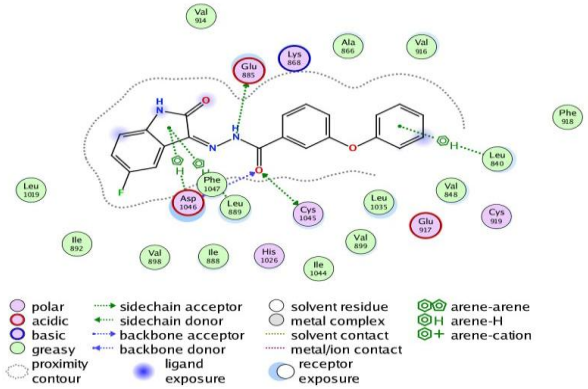

Figure 9: F4 in combination with VEGFR 2 (PDB code: 4ASE) (2D).

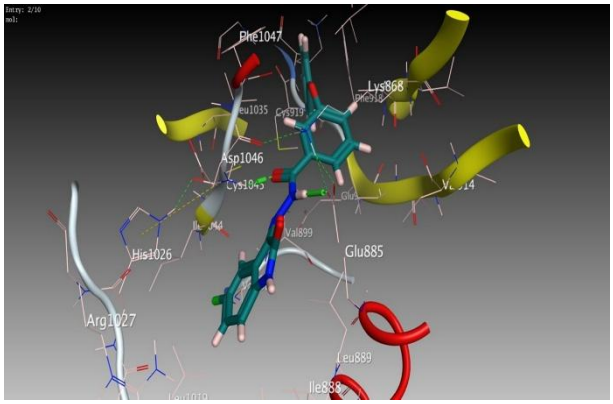

Figure 10: F4 in combination with VEGFR 2 (PDB code: 4ASE) (3D).

IV. CONCLUSION

In this study, we successfully designed and synthesized four novel isatin-based 3-phenoxybenzoic acid derivatives as potential VEGFR-2 inhibitors with anti-angiogenic and anticancer properties. The molecular docking studies provided that these compounds exhibit strong binding affinities to VEGFR-2 by interacting with crucial amino acid residues in the ATP-binding site and the allosteric pocket. These interactions suggest their potential as effective VEGFR-2 inhibitors, comparable or superior to the reference drug sorafenib. The cytotoxic evaluation demonstrated that the synthesized compounds displayed selective anticancer activity against MCF-7 and HepG2 cell lines while exhibiting reduced toxicity toward normal cells (MCF10a and HUVEC). Among the synthesized derivatives, compound F4, which contains a fluorine-substituted isatin core, showed the most potent cytotoxic effects, particularly against MCF-7 cells, while maintaining a high selectivity index. Compounds F1 and F3 exhibited promising activity against HepG2 cells, suggesting their potential as hepatocellular carcinoma-targeting agents. The structure-activity relationship evaluation showed that incorporating an isatin core into the 3-phenoxybenzoic acid scaffold significantly enhanced the binding affinity to VEGFR-2. The presence of specific functional groups, such as the fluorine and methoxy moieties, appeared to influence both potency and selectivity. The docking results supported these findings, highlighting the importance of hydrogen bonding, hydrophobic interactions, and π-π stacking in improving VEGFR-2 inhibition. Our results suggest that these newly synthesized derivatives could serve as promising leads for developing novel VEGFR-2 inhibitors with potential applications in anti-angiogenic cancer therapy. However, further investigations, including in vivo studies, enzymatic inhibition assays, and pharmacokinetic profiling, must validate their efficacy and safety for clinical use. Future research should also optimize these molecules to enhance their potency, selectivity, and drug-like properties. These findings contribute valuable insights into developing VEGFR-2 inhibitors and highlight the potential of isatin-based 3-phenoxybenzoic acid derivatives as a new class of anti-cancer agents targeting tumor angiogenesis.

V.REFERENCES

[1] Al-Rubaye, I. M., & Alibeg, A. A. (2024). Discovery of promising inhibitors for VEGFR-2 using computational methods. *African Journal of Biomedical Research, 27*(3), 582–590.

[2] Alsayad, H. H., Alibeg, A. A., & Oleiwi, Z. K. R. (2024). Molecular docking, synthesis, characterization, and preliminary cytotoxic study of novel 1,2,3-triazole-linked metronidazole derivatives. *Advanced Journal of Chemistry Section A, 7*(6), 797–809.

[3] Alibeg, A. A., & Mohammed, M. H. (2024). Design, synthesis, in silico study and biological evaluation of new isatin-sulfonamide derivatives using mono amide linker as possible histone deacetylase inhibitors. *Polski Merkuriusz Lekarski, 52*(2).

[4] Naji, Z. F., & Naser, N. H. (2025). Synthesis and evaluation of sulfonamide-thiazolidinone conjugates as promising anticancer agents via carbonic anhydrase inhibition. *Wiadomości Lekarskie, 78*(1), 116–129.

[5] Hasan, S. R., & Sahib, A. A. A. (2024). In silico study of new sulfonamide derivatives as possible histone deacetylase inhibitors. *Latin American Journal of Pharmacy, 43*(Special Issue Part 6), 1862–1867.

[6] Alibeg, A. A., & Hussein, T. S. (2024). In silico study of new isatin-sulfonamide derivatives as carbonic anhydrase inhibitors. *Wiadomości Lekarskie, 77*(10).

[7] Alibeg, A. A., & Mohammed, M. H. (2024). Molecular docking, synthesis, characteristics and preliminary cytotoxic study of new coumarin-sulfonamide derivatives as histone deacetylase inhibitors. *Wiadomości Lekarskie, 77*(3).

[8] Saleh, N. M., Abdel-Rahman, A. A. H., Omar, A. M., Khalifa, M. M., & El-Adl, K. (2021). Pyridine-derived VEGFR-2 inhibitors: Rational design, synthesis, anticancer evaluations, in silico ADMET profile, and molecular docking. *Archiv der Pharmazie, 354*(8), 2100085.

[9] Yousef, R. G., Eldehna, W. M., Elwan, A., Abdelaziz, A. S., Mehany, A. B., Gobaara, I. M., et al. (2022). Design, synthesis, in silico and in vitro studies of new immunomodulatory anticancer nicotinamide derivatives targeting VEGFR-2. *Molecules, 27*(13), 4079.

[10] Ran, F., Li, W., Qin, Y., Yu, T., Liu, Z., Zhou, M., et al. (2021). Inhibition of vascular smooth muscle and cancer cell proliferation by new VEGFR inhibitors and their immunomodulator effect: Design, synthesis, and biological evaluation. *Oxidative Medicine and Cellular Longevity, 2021*, 1–21.

[11] Yousef, R. G., Ibrahim, A., Khalifa, M. M., Eldehna, W. M., Gobaara, I. M., Mehany, A. B., et al. (2022). Discovery of new nicotinamides as apoptotic VEGFR-2 inhibitors: Virtual screening, synthesis, anti-proliferative, immunomodulatory, ADMET, toxicity, and molecular dynamic simulation studies. *Journal of Enzyme Inhibition and Medicinal Chemistry, 37*(1), 1389–1403.

[12]Taghour, M. S., Mahdy, H. A., Gomaa, M. H., Aglan, A., Eldeib, M. G., Elwan, A., et al. (2022). Benzoxazole derivatives as new VEGFR-2 inhibitors and apoptosis inducers: Design, synthesis, in silico studies, and antiproliferative evaluation. *Journal of Enzyme Inhibition and Medicinal Chemistry, 37*(1), 2063–2077.

[13] Chung, M. S., & Han, S. J. (2022). Endometriosis-associated angiogenesis and anti-angiogenic therapy for endometriosis. *Frontiers in Global Women's Health, 3*, 856316.

[14] Carmeliet, P. (2003). Angiogenesis in health and disease. *Nature Medicine, 9*, 653–660.

[15] Niu, G., & Chen, X. (2010). *Current Drug Targets, 11*, 1000.

[16] Holmes, K., Roberts, O. L., Thomas, A. M., & Cross, M. J. (2007). *Cellular Signalling, 19*, 2003.

[17] Tugues, S., Koch, S., Gualandi, L., Li, X., & Claesson-Welsh, L. (2011). *Molecular Aspects of Medicine, 32*, 88.

[18] Stuttfeld, E., & Ballmer-Hofer, K. (2009). Structure and function of VEGF receptors. *IUBMB Life, 61*, 915–922.

[19] Lu, R. M., Chiu, C. Y., Liu, I. J., Chang, Y. L., Liu, Y. J., & Wu, H. C. (2019). Novel human Ab against vascular endothelial growth factor receptor 2 shows therapeutic potential for leukemia and prostate cancer. *Cancer Science, 110*, 3773–3787.

[20] Pircher, A., Hilbe, W., Heidegger, I., Drevs, J., Tichelli, A., & Medinger, M. (2011). *International Journal of Molecular Sciences, 12*, 7077.

[21] Abdelgawad, M. A., El-Adl, K., El-Hddad, S. S., Elhady, M. M., Saleh, N. M., Khalifa, M. M., et al. (2022). Design, molecular docking, synthesis, anticancer and anti-hyperglycemic assessments of thiazolidine-2,4-diones bearing sulfonylthiourea moieties as potent VEGFR-2 inhibitors and PPARγ agonists. *Pharmaceuticals, 15*(2), 226.

[22] Eissa, I. H., El-Haggar, R., Dahab, M. A., Ahmed, M. F., Mahdy, H. A., Alsantali, R. I., et al. (2022). Design, synthesis, molecular modeling and biological evaluation of novel benzoxazole-benzamide conjugates via a 2-thioacetamido linker as potential anti-proliferative agents, VEGFR-2 inhibitors and apoptotic inducers. *Journal of Enzyme Inhibition and Medicinal Chemistry, 37*(1), 1587–1599.

[23] Dahab, M. A., Mahdy, H. A., Elkady, H., Taghour, M. S., Elwan, A., Elkady, M. A., et al. (2023). Semi-synthesized anticancer theobromine derivatives targeting VEGFR-2: In silico and in vitro evaluations. *Journal of Biomolecular Structure and Dynamics*, 1–20.

[24] Alsaif, N. A., Mahdy, H. A., Alanazi, M. M., Obaidullah, A. J., Alkahtani, H. M., Al-Hossaini, A. M., et al. (2022). Targeting VEGFR-2 by new quinoxaline derivatives: Design, synthesis, antiproliferative assay, apoptosis induction, and in silico studies. *Archiv der Pharmazie, 355*(2), 2100359.

[25] Mahdy, H. A., Ibrahim, M. K., Metwaly, A. M., Belal, A., Mehany, A. B., El-Gamal, K. M., et al. (2020). Design, synthesis, molecular modeling, in vivo studies and anticancer evaluation of quinazolin-4(3H)-one derivatives as potential VEGFR-2 inhibitors and apoptosis inducers. *Bioorganic Chemistry, 94*, 103422.

[26] Soares, J. X., Afonso, I., Omerbasic, A., Loureiro, D. R. P., Pinto, M. M. M., & Afonso, C. M. M. (2023). The chemical space of marine antibacterials: Diphenyl ethers, benzophenones, xanthones, and anthraquinones. *Molecules, 28*(10), 4073.

[27] Spasov, A. A., Popov, Y. V., Lobasenko, V. S., Korchagina, T. K., Vassiliev, P. M., & Kuznetsova, V. A. (2017). Synthesis and pharmacological activity of 3-phenoxybenzoic acid derivatives. *Russian Journal of Bioorganic Chemistry, 43*(2), 163–169.

[28] Chaudhari, P., Bari, S., Surana, S., Shirkhedkar, A., Wakode, S., Shelar, S., et al. (2022). Logical synthetic strategies and structure–activity relationship of indolin-2-one hybrids as small molecule anticancer agents: An overview. *Journal of Molecular Structure, 1247*, 131280.

[29] Moffat, A. C., Osselton, M. D., Widdop, B., & Watts, J. (2011). *Clarke's Analysis of Drugs and Poisons*. London: Pharmaceutical Press.

[30] Abbas, A. H., Mahmood, A. A. R., Tahtamouni, L. H., Al-Mazaydeh, Z. A., Rammaha, M. S., Alsoubani, F., et al. (2021). A novel derivative of picolinic acid induces endoplasmic reticulum stress-mediated apoptosis in

human non-small cell lung cancer cells: Synthesis, docking study, and anticancer activity. *Pharmacia, 68*(3), 679–692.

[31] Naser, N. H., Alibeg, A. A., & AbdAl-Zahra, A. J. (2022). Design, synthesis, in silico study and preliminary pharmacological evaluation of ibuprofen derivatives containing 1,3,4-oxadiazole moiety. *Materials Today: Proceedings*. https://doi.org/10.1016/j.matpr.2022.05.092

[32] Faisal, M., & Raauf, A. (2015). Design, synthesis, and acute anti-inflammatory evaluation of new non-steroidal anti-inflammatory agents having 4-thiazolidinone pharmacophore. *Journal of Natural Sciences Research, 5*(6), 21–28.

[33] Naji, Z. F., & Naser, N. H. (2024). In silico study of five new sulfonamide derivatives bearing a thiazolidine-4-one moiety: Targeting carbonic anhydrase IX. *Reviews in Clinical Pharmacology and Pharmacokinetics: International Edition, 38*, 161–173.